SUPERPARAMAGNETIC LANTHANIDE (La^{3+}, Gd^{3+}, Nd^{3+}) DOPED *Mn-Zn* FERRITE NANOPARTICLES: EFFECT OF DOPANT CONTENT

SYNOPSIS

Submitted for the partial fulfillment of the requirement for the degree of

DOCTOR OF PHILOSOPHY

By

PRASHANT THAKUR

DEPARTMENT OF PHYSICS AND MATERIALS SCIENCE

JAYPEE UNIVERSITY OF INFORMATION TECHNOLOGY
WAKNAGHAT, DISTRICT SOLAN, H.P., INDIA

OCTOBER 2018

CONTENTS

1. Introduction
2. Objectives of the work
   2.1 Optimization of sintering temperature for $Mn_{0.5}Zn_{0.5}Fe_2O_4$ nano ferrites
   2.2 Structural and morphological study of La^{3+}, Gd^{3+}, Nd^{3+} doped *Mn-Zn* ferrites
   2.3 Cation distribution and magnetic study of La^{3+}, Gd^{3+}, Nd^{3+} doped *Mn-Zn* nano ferrites
3. Conclusion
4. References
5. List of Publications

1. Introduction

Over the last few years spinel ferrites have shown their competence in various technological applications like high-frequency devices, catalysis, microwave devices etc. [1-5]. These materials have also shown their usefulness in biomedical applications particularly for hyperthermia and drug delivery [6, 7]. Spinel ferrites exist in AB_2O_4 form with *A* as divalent metal ions (*e.g.* Mn^{2+}, Co^{2+}, Zn^{2+}, Mg^{2+}, Ni^{2+}*etc*.) and *B* as trivalent metal ions {*e.g.* rare earth metals (La^{3+}, Gd^{3+}*etc*.), In^{3+}, Al^{3+}*etc*.}. The places occupied by *A* ions are known as tetrahedral sites and the places occupied by *B* ions are known as octahedral sites. The distribution of ions in these sites is responsible for the different properties of spinel ferrites [1]. The structural, electrical and magnetic properties of spinel ferrites are being governed by their chemical composition, synthesis technique, type of dopant and particle size [2].

Among various soft ferrites, manganese-zinc spinel ferrites have shown their importance due to their application in high frequency devices and the property of high initial magnetic permeability [8,9]. The magnetic properties of manganese-zinc spinel ferrites have shown their dependence on sintering temperature, sintering time, particle size, microstructure, etc. [8]. Manganese-zinc spinel ferrites are widely used in computer memory chips, antenna rods, electromagnetic interference devices, transformer cores, microwave devices, radio frequency coils and some other devices of microelectronics due to some of their unique properties [8]. Different synthesis techniques *viz*. sol−gel, sol−gel autocombustion, hydrothermal, co-precipitation *etc*. have been employed by various researchers to prepare manganese-zinc spinel ferrites [6,10-21]. Evolution of microstructure and homogeneous compositions on mixing the precursors at molecular stage are the primary advantages of these synthesis techniques [10-20].

Addition of lanthanide elements to manganese-zinc spinel ferrites has shown large magnetic moments, magnetostriction and magnetocrystalline anisotropy at low temperatures [22]. The localized 4*f* electrons and strong spin-orbit coupling of the angular momentum of rare earth ions are mainly causative for the appearance of these prominent properties in manganese-zinc spinel ferrites [22]. Further, a shielding is provided to 4*f* electrons by $5s^2$ and $5p^6$ shells and this leads to make a little effect of potential field of surrounding ions on the 4*f* electrons. There is migration of some divalent metal ions from octahedral (B) site to the tetrahedral (A) site with the substitution of the rare earth ions in spinel ferrite. Migration of metal ions from octahedral (B)

site to the tetrahedral (A) site also depends upon the size of ionic radii in spinel ferrite [22]. It is difficult to put in the lanthanide ions (RE^{3+}) into the spinel structure of ferrite owing to their large ionic radii via classical ceramic method [1]. Therefore, co-precipitation technique has been employed for the synthesis of RE^{3+} doped manganese-zinc spinel nano ferrites [1].

2. Objectives of the work

2.1 Objective 1:

Optimization of sintering temperature for $Mn_{0.5}Zn_{0.5}Fe_2O_4$ nano ferrites

- **Synthesis and characterization of $Mn_{0.5}Zn_{0.5}Fe_2O_4$ nano ferrites**

Co-precipitation synthesis technique has been employed for the synthesis of $Mn_{0.5}Zn_{0.5}Fe_2O_4$ ferrite powder. The starting materials, manganese chloride, zinc chloride, iron (III) chloride and *NaOH* have been procured from Merck India (98% purity) and are used as received. For the synthesis of $Mn_{0.5}Zn_{0.5}Fe_2O_4$ nanoferrites, a schematic diagram has been depicted in figure 1.

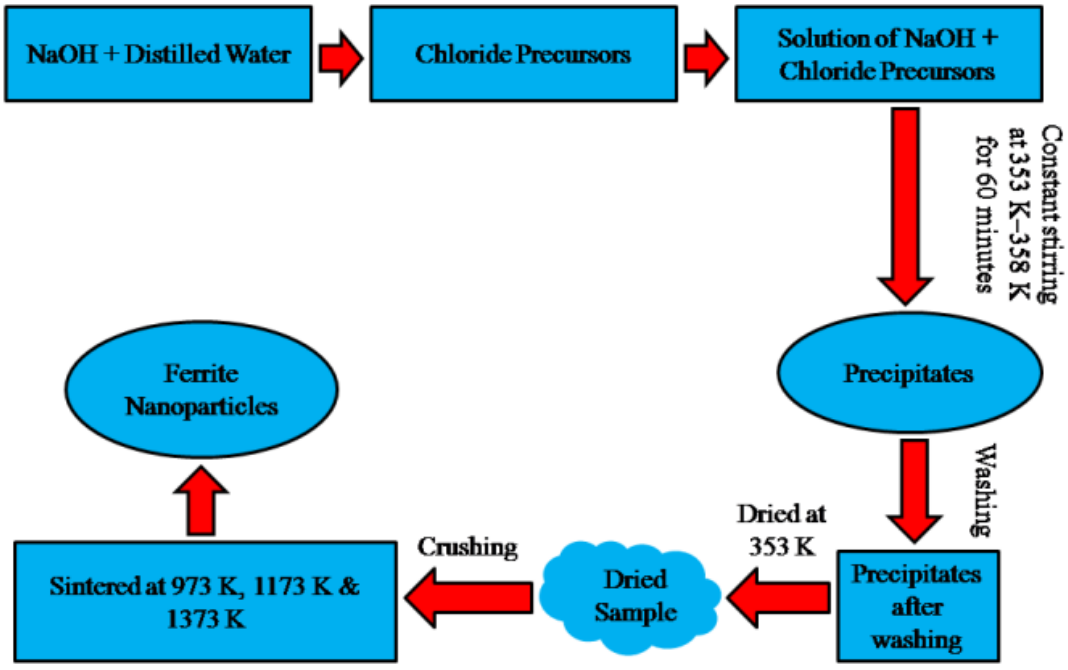

Figure 1: Schematic diagram for preparation of $Mn_{0.5}Zn_{0.5}Fe_2O_4$ ferrite powder.

In 60 ml of distilled water, 3M solution (0.5M manganese chloride + 0.5M zinc chloride +2M iron (III) chloride) of starting materials has been prepared (say stock 1). In 100 ml of distilled water, 4M *NaOH* solution has been prepared (say stock 2). The stock 1 has been poured into the

boiling solution of *NaOH* under stirring. The value of pH has been held at 11 to 12 throughout the co-precipitation. The reaction has been put to force at 353 K–358 K temperature for an hour under energetic stirring. The obtained precipitates have been left to settle at room temperature. The obtained precipitates have been washed several times with double distilled water followed by overnight drying in a hot air oven at 353 K. The dried sample has been crushed to powder with the help of mortar and pestle. Some of the dried powdered sample has been divided into three parts and subjected to different sintering temperatures *i.e.* 973 K, 1173 K and 1373 K. After sintering, the samples have been characterized using X-ray diffraction (XRD), field emission scanning electron microscopy (FE-SEM) and Fourier transform infrared spectroscopy (FTIR).

❖ Results and discussion

The synthesized ferrite has been subjected to sintering sample at three temperatures i.e. 973 K, 1173 K and 1373 K. From the structural analysis using XRD at three sintering temperatures, a single phase cubical spinel has been observed at 1373 K whereas a secondary phase Fe_2O_3 has been observed at lower sintering temperatures. XRD graphs of $Mn_{0.5}Zn_{0.5}Fe_2O_4$ nano ferrites sintered at three different temperatures have been given in figure 2.

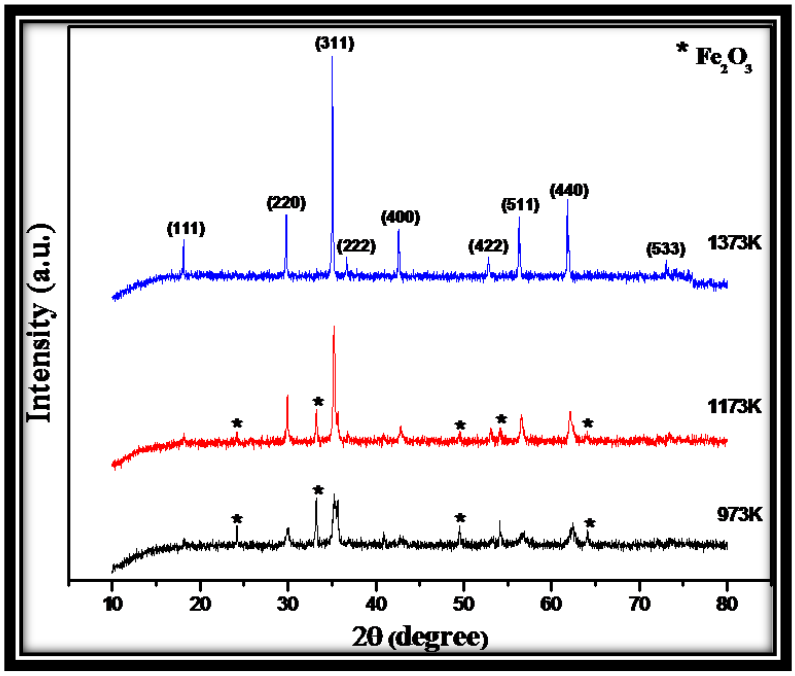

Figure 2: XRD graphs of sintered $Mn_{0.5}Zn_{0.5}Fe_2O_4$ nano ferrites (at 973 K, 1173 K and 1373 K)

The average crystallite size has been found to increase (11.38 nm to 67.42 nm) with the increasing sintering temperature (973 K to 1373 K). The presence of two absorption bands (421 cm^{-1} - 491 cm^{-1} and 516 cm^{-1} - 592 cm^{-1}) in FTIR spectra have supported the formation of spinel ferrite. FTIR spectra of $Mn_{0.5}Zn_{0.5}Fe_2O_4$ nano ferrites sintered at three different temperatures have been shown in figure 3.

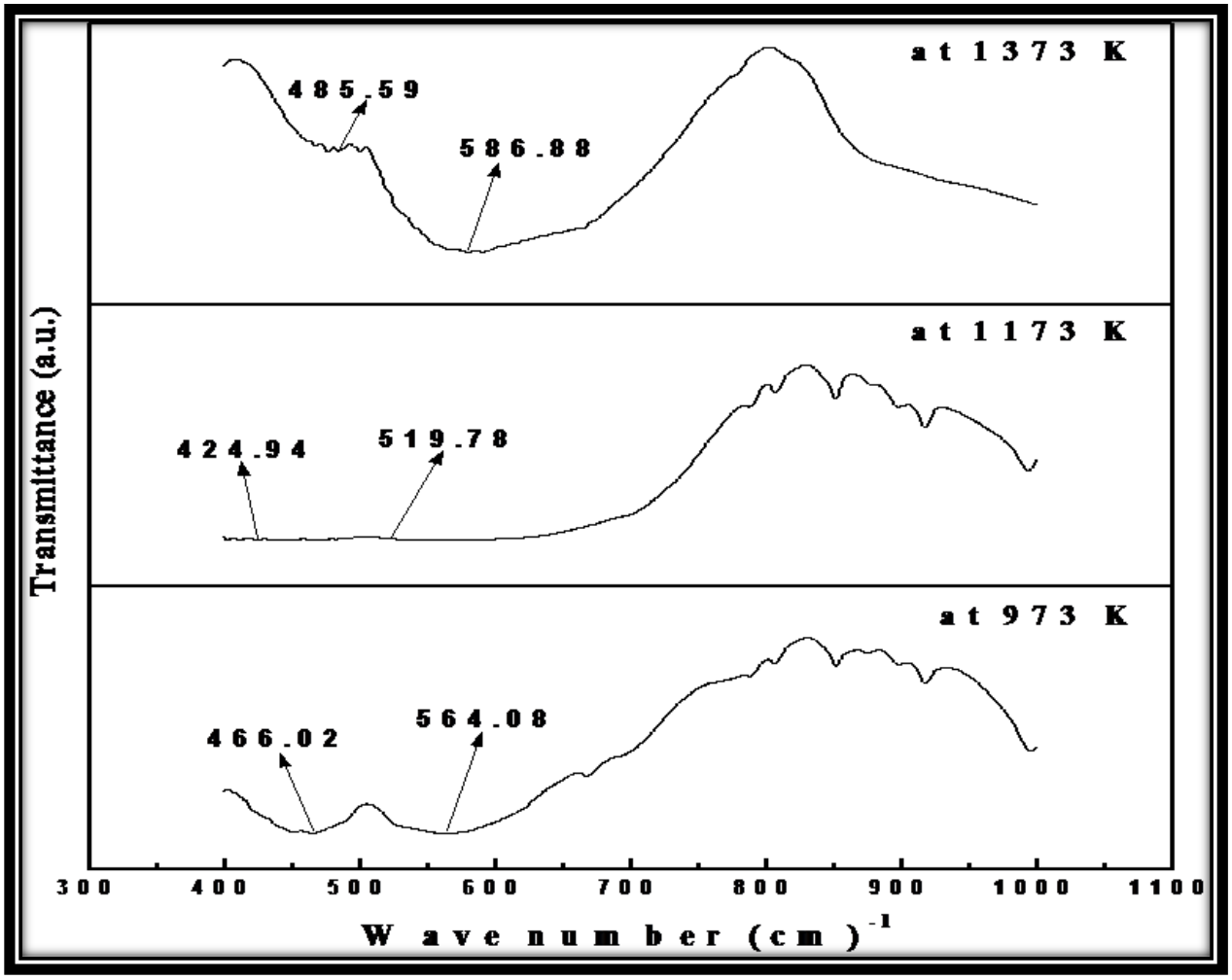

Figure 3: FTIR spectra of $Mn_{0.5}Zn_{0.5}Fe_2O_4$ sample sintered at 973 K, 1173 K and 1373 K.

FE-SEM images have shown the formation of homogenous crystalline nanoparticles with increase in sintering temperature. FE-SEM images of $Mn_{0.5}Zn_{0.5}Fe_2O_4$ nano ferrites sintered at three different temperatures have been presented in figure 4.

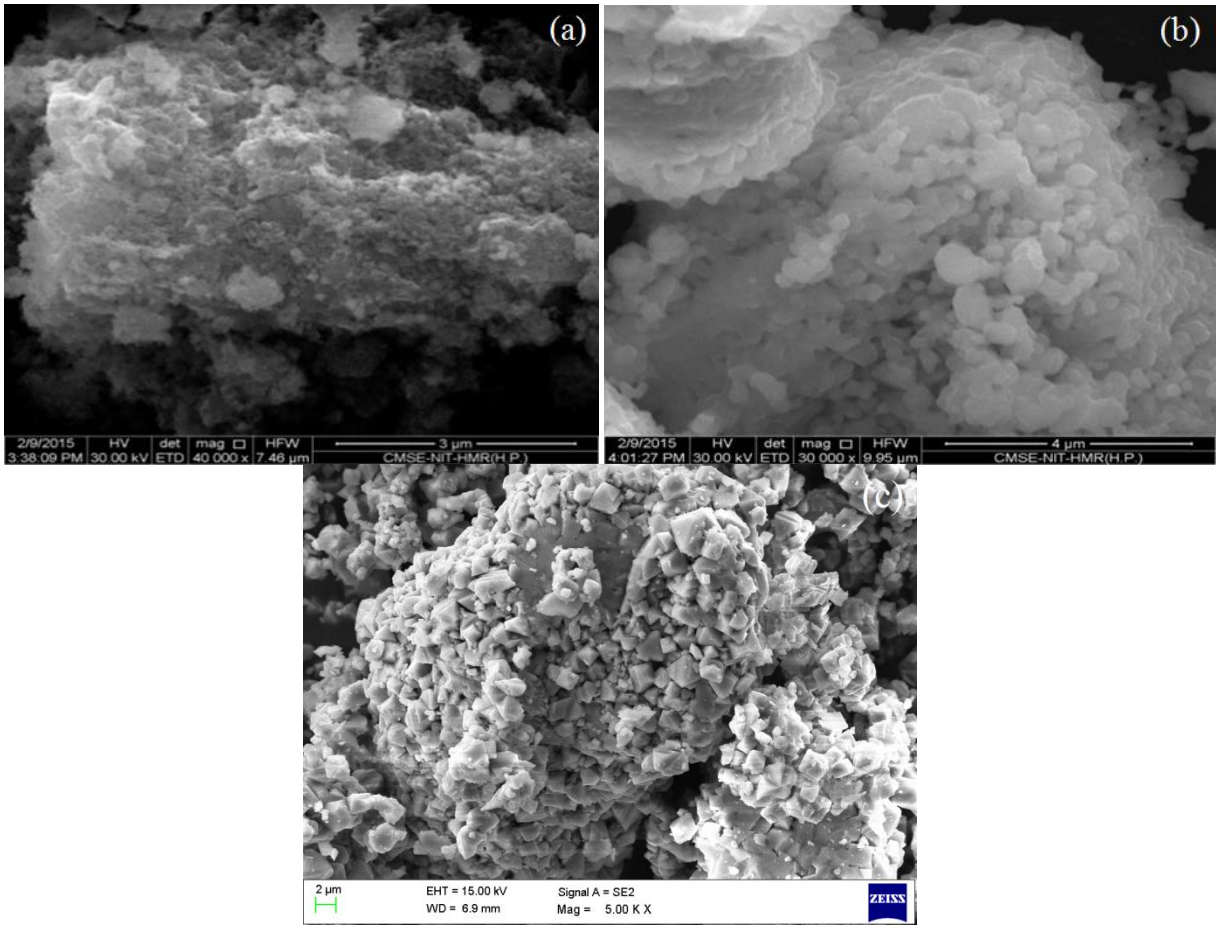
(a)
(b)
(c)
2/9/2015 3:38:09 PM HV 30.00 kV det ETD mag 40 000 x HFW 7.46 µm 3 µm CMSE-NIT-HMR(H.P.)
2/9/2015 4:01:27 PM HV 30.00 kV det ETD mag 30 000 x HFW 9.95 µm 4 µm CMSE-NIT-HMR(H.P.)
2 µm
EHT = 15.00 kV
WD = 6.9 mm
Signal A = SE2
Mag = 5.00 K X
ZEISS

Figure 4: FESEM images of $Mn_{0.5}Zn_{0.5}Fe_2O_4$ sample sintered at (a) 973 K (b) 1173 K (c) 1373 K

Considering these results, we have taken the sintering temperature as 1373 K for further investigation of lanthanide doped *Mn-Zn* ferrites.

2.2 Objective 2:

Structural and morphological study of La^{3+}, Gd^{3+}, Nd^{3+} doped *Mn-Zn* ferrites

- **Synthesis and characterizations of La^{3+}, Gd^{3+}, Nd^{3+} doped *Mn-Zn* nano ferrites**

In this research work, magnetic nanoparticles of lanthanide (*RE = La, Gd, Nd*) doped *Mn-Zn* ferrites have been prepared using the co-precipitation synthesis technique. Schematic diagram for the synthesis of lanthanide (*RE*) doped *Mn-Zn* ferrites has been shown in Figure 5. To synthesize a composition, the chloride precursors are used and have been taken in solution form. Solution of chloride as starting materials has been poured into solution of *NaOH* under

constant stirring at 80 °C±5°C for 60 minutes. The pH of solution has been maintained at 11- 12 during the precipitation of particles. The precipitates are collected, washed a number of times and then dried overnight at 80 °C in a hot air oven. After this, the dried precipitates are crushed to powder form and sintered at 1373 K for 3 hrs. Planned chemical reaction for the synthesis of $Mn_{0.5}Zn_{0.5}RE_xFe_{2-x}O_4$ spinel nano ferrites, where x=0, 0.025, 0.050, 0.075, 0.1, has been given below;

$$0.5(MnCl_2) + 0.5(ZnCl_2) + x(RECl_3) + (2-x)(FeCl_3) + 4NaOH \xrightarrow{Synthesis\ at\ 353K\ for\ 60\ minutes} Mn_{0.5}Zn_{0.5}RE_xFe_{(2-x)}O_4 + 4NaCl + 2H_2\uparrow + 2Cl_2\uparrow \quad \text{(Step 1)}$$

$$Mn_{0.5}Zn_{0.5}RE_xFe_{(2-x)}O_4 + 4NaCl \xrightarrow{After\ washing} Mn_{0.5}Zn_{0.5}RE_xFe_{(2-x)}O_4 + NaCl \quad \text{(Step 2)}$$

$$Mn_{0.5}Zn_{0.5}RE_xFe_{(2-x)}O_4 + NaCl \xrightarrow{Sintered\ at\ 1373K} Mn_{0.5}Zn_{0.5}RE_xFe_{(2-x)}O_4(Ferrite) \quad \text{(Step 3)}$$

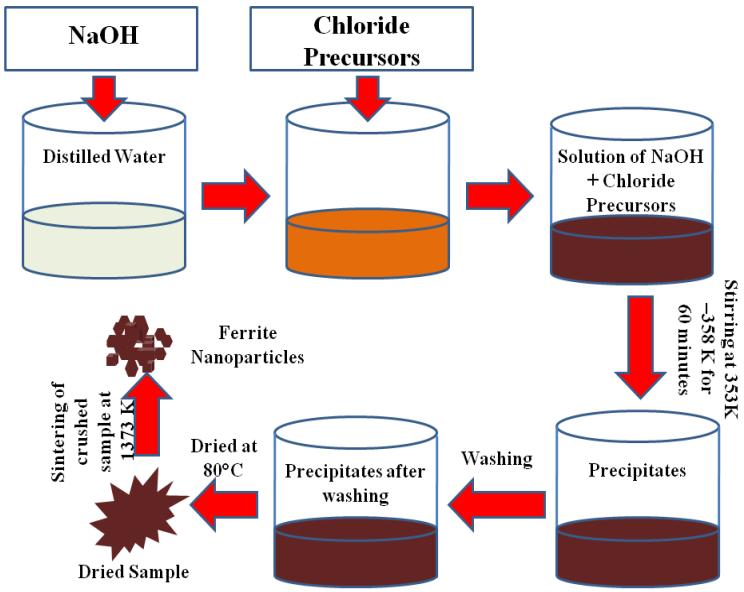

Figure 5: Schematic diagram of co-precipitation technique for the synthesis of lanthanide (*RE = La, Gd, Nd*) doped *Mn-Zn* ferrites.

The sintered samples have been characterized by X-ray diffraction (XRD), Fourier transform infrared spectra (FTIR), field emission scanning electron microscope (FE-SEM) and energy dispersive X-Ray spectroscopy (EDS).

❖ Results and discussion

Cubic spinel phase has been observed for $Mn_{0.5}Zn_{0.5}RE_xFe_{2-x}O_4$ (x = 0, 0.025, 0.050, 0.075, 0.1) nano ferrites synthesized through co-precipitation synthesis technique. XRD graphs of prepared $Mn_{0.5}Zn_{0.5}RE_xFe_{2-x}O_4$ nano ferrites have been presented in figure (6, 7 & 8).

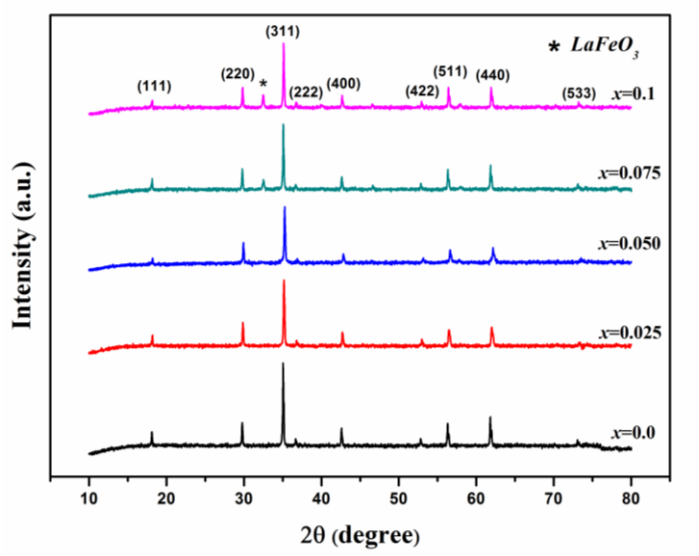

Figure 6: XRD graphs of $Mn_{0.5}Zn_{0.5}La_xFe_{2-x}O_4$ ferrites.

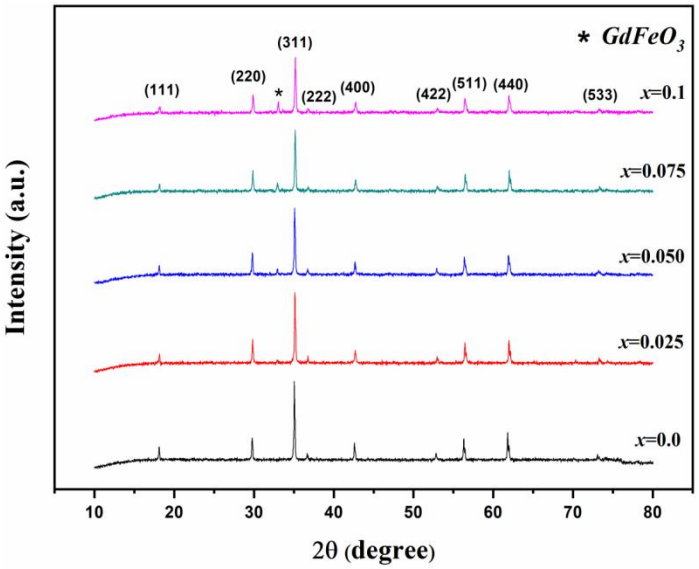

Figure 7: XRD graphs of $Mn_{0.5}Zn_{0.5}Gd_xFe_{2-x}O_4$ ferrites.

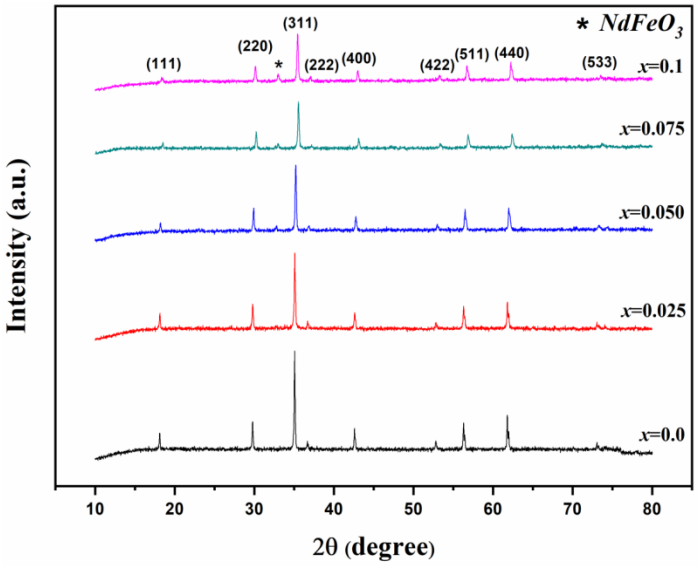

Figure 8: XRD spectra of $Mn_{0.5}Zn_{0.5}Nd_xFe_{2-x}O_4$ ferrites.

For the three dopants used in *Mn-Zn* ferrites, the crystallite size, lattice constant, interplanar spacing and packing factor have been observed to decrease generally. FTIR spectra of prepared *Gd* doped *Mn-Zn* nano ferrites have been shown in figure 9. Occurrence of spinel structure in all the investigated samples has been confirmed from FTIR spectroscopy.

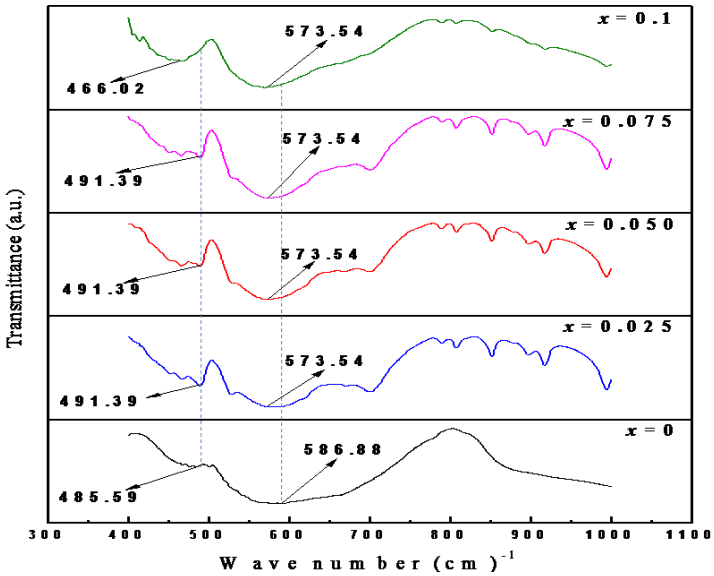

Figure 9: FTIR spectra of $Mn_{0.5}Zn_{0.5}Gd_xFe_{2-x}O_4$ nano ferrites. The y-axis scale has been shifted for clarity.

A clear shift in the position of absorption bands with *RE* (= *La*, *Gd* & *Nd*) doping has also been observed. FE-SEM micrographs of $Mn_{0.5}Zn_{0.5}RE_xFe_{2-x}O_4$ (where *RE=La*, *Gd*, *Nd*) ferrites show

sharp crystalline structures. EDS spectroscopy confirms the presence of constituent elements *Mn*, *Zn*, *RE* (= *La*, *Gd* & *Nd*), *Fe*, *O* in all the investigated samples.

2.3 Objective 3:
Cation distribution and magnetic study of La^{3+}, Gd^{3+}, Nd^{3+} doped *Mn-Zn* nano ferrites

❖ Synthesis and characterizations of La^{3+}, Gd^{3+}, Nd^{3+} doped *Mn-Zn* nano ferrites

RE^{3+} (La^{3+}, Gd^{3+}, Nd^{3+}) doped manganese - zinc ferrites have been prepared using co-precipitation method. Preparation of samples has been described in section 2.2. The sintered samples have been characterized with vibrating sample magnetometer (VSM; PAR-155) in a magnetic field range −10 *kOe* to +10 *kOe* at room temperature. Some important theoretical parameters have also been calculated for all prepared samples of $Mn_{0.5}Zn_{0.5}RE_xFe_{2-x}O_4$ (x=0, 0.025, 0.050, 0.075 and 0.1) nano ferrites using cation distribution.

❖ Results and discussion

From the proposed cation distribution, at the tetrahedral sites Zn^{2+}ions and Fe^{3+} ions have A-A exchange interactions whereas at the octahedral sites Mn^{2+} ions, Fe^{3+}ions and RE^{3+}(= La^{3+}, Gd^{3+} & Nd^{3+}) ions have B-B interactions. Both bivalent (Zn^{2+} & Mn^{2+}) and trivalent (Fe^{3+} & RE^{3+}) metal ions at the tetrahedral and octahedral sites have A-B super exchange interactions.

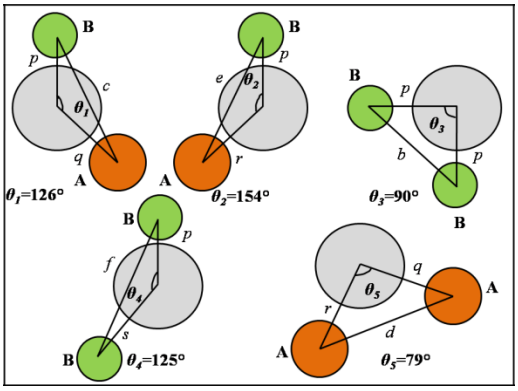

Figure 10: Interionic distances and the angles between the ions in spinel ferrites.

This has been further confirmed by the bond angles between the metal ions. These bond angles and interionic distances between metal ions and also with anions have been shown in figure 10. There is an increase in the values of θ_1, θ_2, θ_5 suggesting strong A-A and A-B interactions whereas a decrease in the values of θ_3 and θ_4 indicates weak B-B interactions. M-H curves of prepared $Mn_{0.5}Zn_{0.5}RE_xFe_{2-x}O_4$ nano ferrites have been presented in figure (11, 12 & 13).

Magnetic characterizations show superparamagnetic and paramagnetic behaviour of RE^{3+} (= La^{3+}, Gd^{3+}, Nd^{3+}) doped *Mn-Zn* spinel ferrite. The absence of retentivity (*Mr*) and coercivity (*Hc*) at zero magnetic field has been observed for all the samples under investigation.

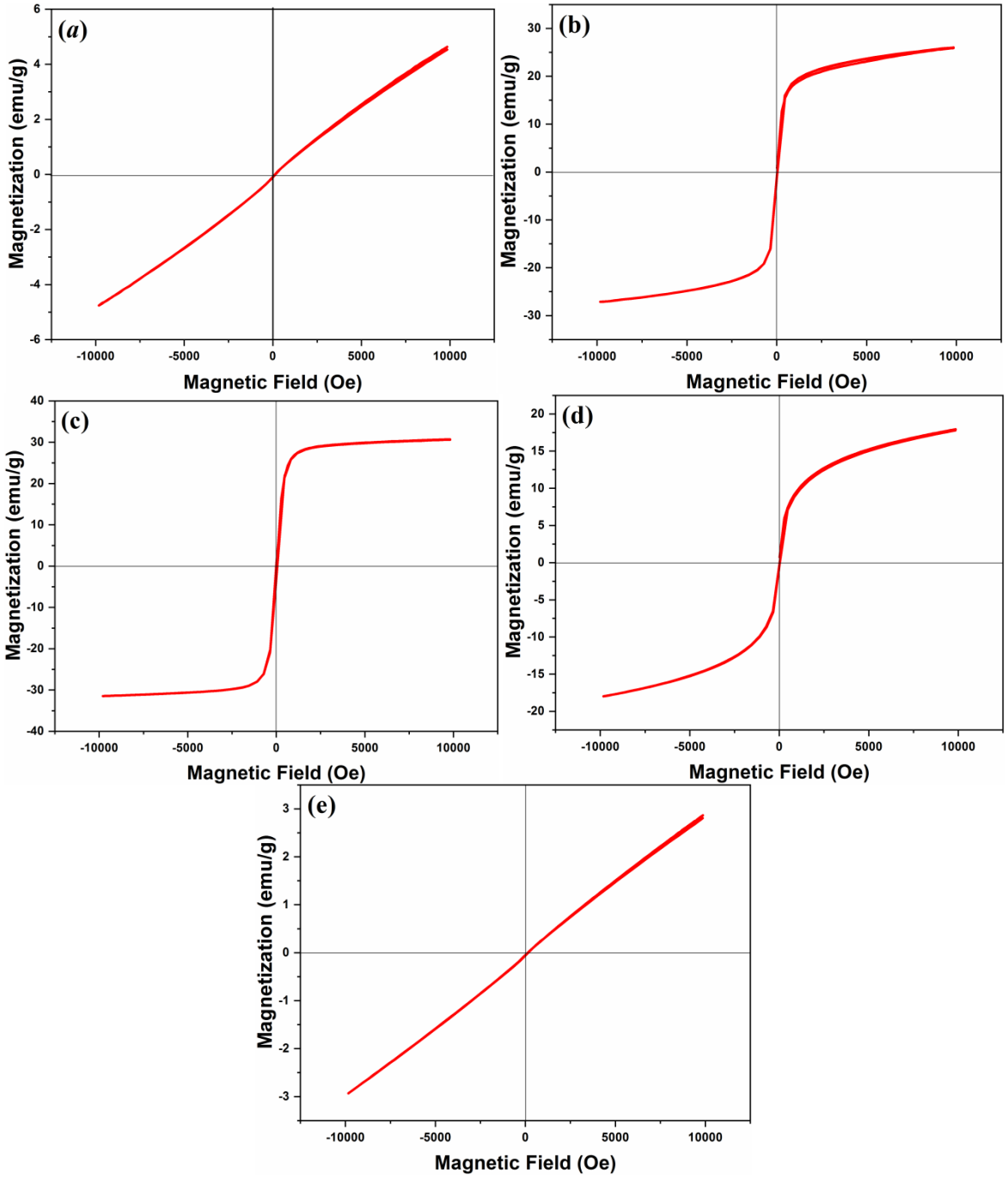

Figure 11(*a*-e): M-H curve of $Mn_{0.5}Zn_{0.5}La_xFe_{2-x}O_4$ (x = 0, 0.025, 0.050, 0.075 and 0.1) nano ferrites

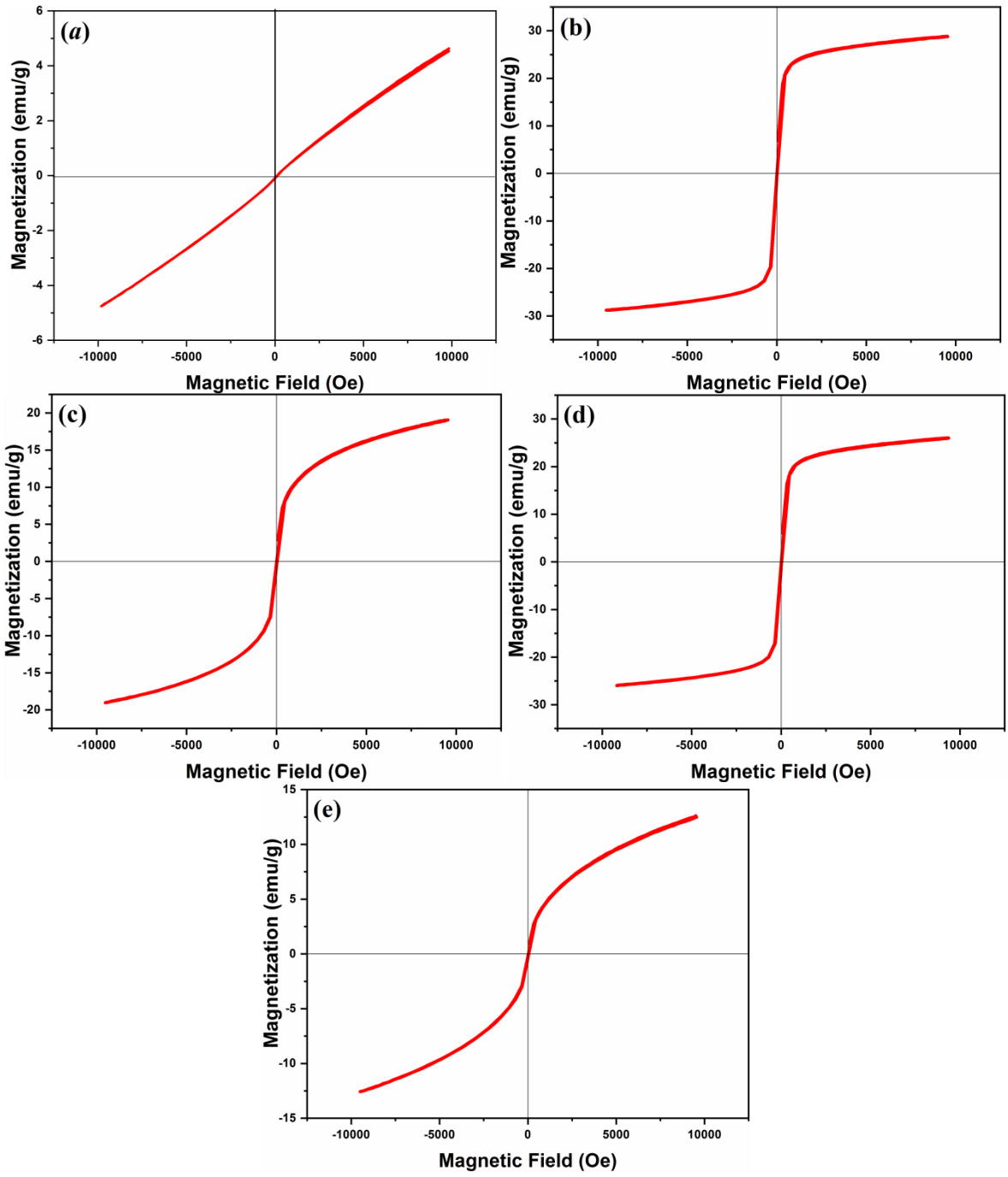

Figure 12(*a*-e): M-H curve of $Mn_{0.5}Zn_{0.5}Gd_xFe_{2-x}O_4$ (x = 0, 0.025, 0.050, 0.075 and 0.1) nano ferrites

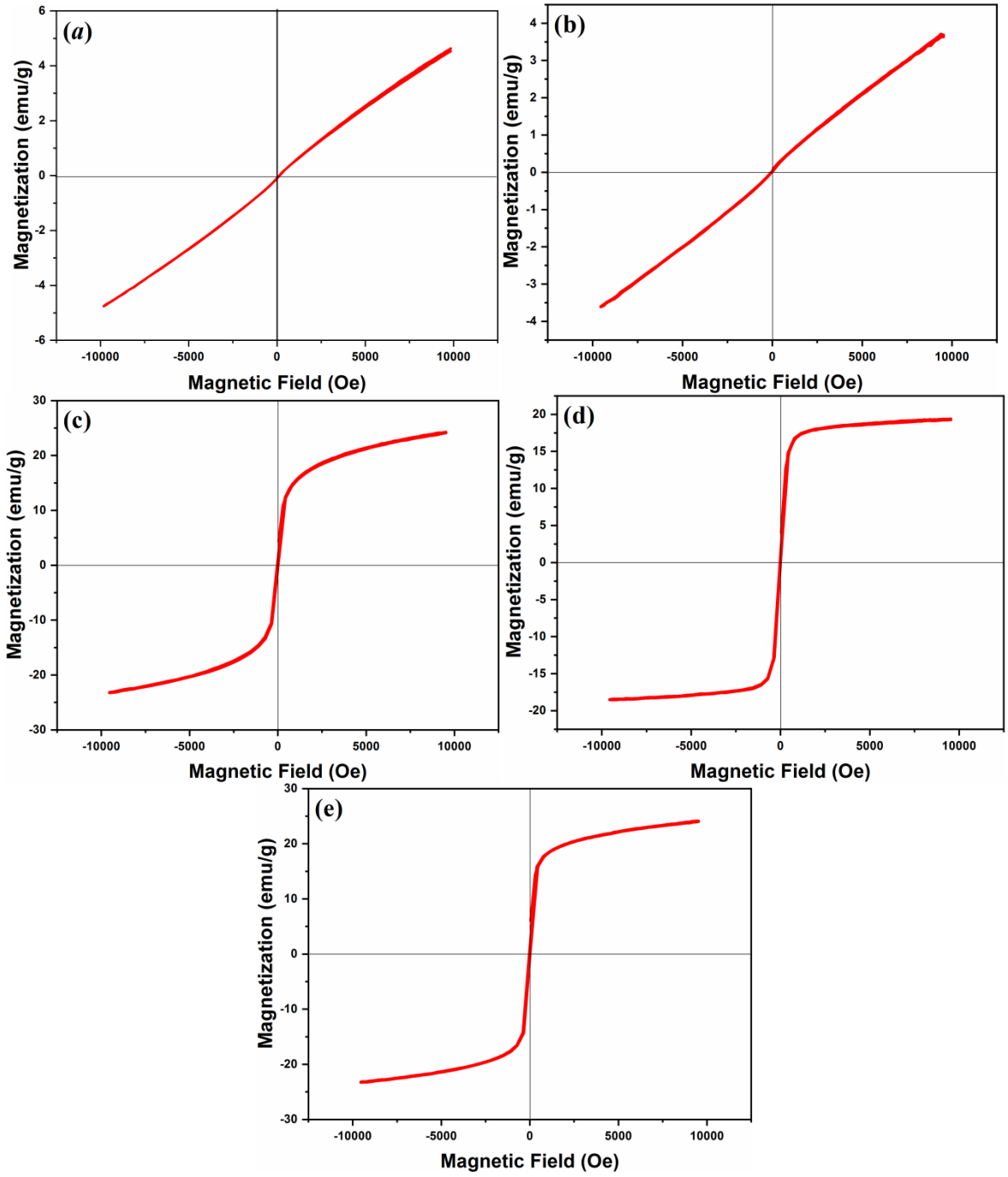

Figure 13(*a*-e): M-H curve of $Mn_{0.5}Zn_{0.5}Nd_xFe_{2-x}O_4$ (x = 0, 0.025, 0.050, 0.075 and 0.1) nano ferrites

The increase in magnetic parameters (M_S and n_B) with RE^{3+} doping is correlated with the bond angles. For La^{3+} (x = 0.050), Gd^{3+} (x = 0.025) and Nd^{3+} (x = 0.1) compositions, a maximum value of magnetic parameters have been observed.

3. Conclusion

The co-precipitation synthesis technique has been used for the preparation of $Mn_{0.5}Zn_{0.5}Fe_2O_4$ ferrite. The synthesized ferrite has been subjected to sintering sample at three temperatures i.e. 973 K, 1173 K and 1373 K. From the structural analysis using XRD at three sintering temperatures, a single phase cubical spinel has been observed at 1373 K whereas a secondary phase Fe_2O_3 has been observed at lower sintering temperatures. The average crystallite size has been found to increase (11.38 nm to 67.42 nm) with the increasing sintering temperature (973 K to 1373 K). The presence of two absorption bands (421 cm^{-1} - 491 cm^{-1} and 516 cm^{-1} - 592 cm^{-1}) in FTIR spectra has supported the formation of spinel ferrite. FE-SEM images have shown the formation of homogenous crystalline nanoparticles with increase in sintering temperature. Considering these results, we have taken the sintering temperature as 1373 K for further investigation of doped Mn-Zn ferrites.

Structural investigations have shown cubic spinel phase for $Mn_{0.5}Zn_{0.5}RE_xFe_{2-x}O_4$ (x = 0, 0.025, 0.050, 0.075, 0.1) nano ferrites synthesized through co-precipitation synthesis technique, where *RE = La, Gd & Nd*. For the three dopants used in *Mn-Zn* ferrites, the crystallite size, lattice constant, interplanar spacing and packing factor have been observed to decrease generally. The occurrence of spinel structure in all the investigated samples has also been confirmed from FTIR spectroscopy. A clear shift in the position of absorption bands with *RE* (= *La*, *Gd* & *Nd*) doping has also been observed. FESEM micrographs of $Mn_{0.5}Zn_{0.5}RE_xFe_{2-x}O_4$ (where *RE = La, Gd, Nd*) ferrites show sharp crystalline structures. EDS spectroscopy confirms the presence of constituent elements *Mn, Zn, RE* (= *La*, *Gd* & *Nd*), *Fe, O* in all the investigated samples.

From the proposed cation distribution, at the tetrahedral sites Zn^{2+} ions and Fe^{3+} ions have A-A exchange interactions whereas at the octahedral sites Mn^{2+} ions, Fe^{3+} ions and RE^{3+} (= La^{3+}, Gd^{3+} & Nd^{3+}) ions have B-B interactions. Both divalent (Zn^{2+} & Mn^{2+}) and trivalent (Fe^{3+} & RE^{3+}) metal ions at the tetrahedral and octahedral sites have A-B super exchange interactions. This has been further confirmed by the bond angles between the metal ions. There is an increase in the values of θ_1, θ_2, θ_5 suggesting strong A-A and A-B interactions whereas a decrease in the values of θ_3 and θ_4 indicates weak B-B interactions. Magnetic characterizations show superparamagnetic and paramagnetic behaviour of RE^{3+} (= La^{3+}, Gd^{3+}, Nd^{3+}) doped *Mn-Zn* spinel ferrite. The absence of retentivity (*Mr*) and coercivity (*Hc*) at zero magnetic field has been observed for samples under investigation. The increase in magnetic parameters (M_S and n_B) with

RE^{3+} doping is correlated with the bond angles. For La^{3+} (x = 0.050), Gd^{3+} (x = 0.025) and Nd^{3+} (x = 0.1) compositions, a maximum value of magnetic parameters have been observed. The ferrite nanoparticles having superparamagnetic behaviour may have several applications in biomedicine like drug delivery, gene delivery, MRI contrast enhancement, hyperthermia, radionuclide delivery *etc*.

4. References

[1] P. Samoila, L. Sacarescu, A.I. Borhan, D. Timpu, M. Grigoras, N. Lupu, M. Zaltariov, V. Harabagiu, Magnetic properties of nanosized Gd doped Ni–Mn–Cr ferrites prepared using the sol–gel autocombustion technique, Journal of Magnetism and Magnetic Materials 378 (2015) 92-97.

[2] G.Dixit, J.P. Singh, R.C. Srivastava, H.M. Agrawal, Magnetic resonance study of Ce and Gd doped $NiFe_2O_4$ nanoparticles, Journal of Magnetism and Magnetic Materials 324 (2012) 479–483.

[3] M.A. Iqbal, M.Islam, M.N.Ashiq, I. Ali, A. Iftikhar, H.M. Khan, Effect of Gd-sub- stitiution on physical and magnetic properties of $Li_{1.2}Mg_{0.4}Gd_xFe_{(2-x)}O_4$ ferrites, Journal of Alloys and Compounds 579 (2013) 181–186.

[4] P. Samoila, T. Slatineanu, P. Postolache, A.R. Iordan, M.N. Palamaru, The effect of chelating/combustion agent on catalytic activity and magnetic properties of Dy doped Ni–Zn ferrite, Materials Chemistry and Physics 136 (2012) 241–246.

[5] A.I. Borhan, P. Samoila, V. Hulea, A.R. Iordan, M.N. Palamaru, Effect of Al^{3+} sub-stituted zinc ferrite on photocatalytic degradation of Orange I azo dye, Journal of Photochemistry and Photobiology A: Chemistry 279 (2014) 17–23.

[6] I. Sharifi, H. Shokrollahi, S. Amiri, Ferrite-based magnetic nano fluids used in hyperthermia applications, Journal of Magnetism and Magnetic Materials 324 (2012) 903–915.

[7] T.N. Brusentsova, V.D. Kuznetsov, Synthesis and investigation of magnetic properties of substituted ferrite nanoparticles of spinel system $Mn_{1-x}Zn_x[Fe_{2-y}L_y]O_4$, Journal of Magnetism and Magnetic Materials 311 (2007) 22–25.

[8] Katarzyna Winiarska, Irena Szczygieł, and Roman Klimkiewicz, Manganese–zinc ferrite synthesis by the sol–gel autocombustion method. Effect of the precursor on the ferrite's catalytic properties, Industrial & Engineering Chemistry Research 52 (2012) 353−361.

[9] Alex. Goldman, Modern ferrite technology. Springer Science & Business Media, 2006.

[10] J. Azadmanjiri, Preparation of Mn−Zn ferrite nanoparticles from chemical sol−gel combustion method and the magnetic properties after sintering, Journal of Non-Crystalline Solids, 353 (2007)4170-4173.

[11] H. Waqas, A. H. Qureshi, Low temperature sintering study of nanosized Mn−Zn ferrites synthesized by sol−gel autocombustion process, Journal of thermal analysis and calorimetry 100 (2010) 529-535.

[12] I. Szczygiel, K. Winiarska, Low-temperature synthesis and characterization of the Mn−Zn ferrite, Journal of thermal analysis and calorimetry 104 (2011) 577-583.

[13] A. C. F. M. Costa, V. J. Silva, C. C. Xin, D. A. Vieira, D. R. Cornejo, R. H. G. A. Kiminami, Effect of urea and glycine fuels on the combustion reaction synthesis of Mn−Zn ferrites: Evaluation of morphology and magnetic properties, Journal of Alloys and Compounds 495 (2010) 503-505.

[14] R. V. Mangalaraja, S. Ananthakmar, P. Manohar, F. D. Gnanam, M. Awano, Characterization of $Mn_{0.8}Zn_{0.2}Fe_2O_4$ synthesized by flash combustion technique, Materials Science and Engineering: A 367 (2004) 301-305.

[15] R. Arulmurugan, G. Vaidyanathan, S. Sendhilnathan, B. Jeyadevan, Mn−Zn ferrite nanoparticles for ferrofluid preparation: Study on thermal−magnetic properties, Journal of Magnetism and Magnetic Materials 298 (2006) 83-94.

[16] X. Cao, G. A. Liu, Y. M. Wang, J. H. Li, R. Y. Honga, Preparation of octahedral shaped $Mn_{0.8}Zn_{0.2}Fe_2O_4$ ferrites via coprecipitation, Journal of Alloys and Compounds 497 (2010) L9-L12.

[17] C. Rath, K. K. Sahu, S. Anand, S. K. Date, N. C. Mishra, R. P. Das, Preparation and characterization of nanosize Mn−Zn ferrite, Journal of magnetism and magnetic materials 202 (1999) 77-84.

[18] L. Nalbandian, A. Delimitis, V. T. Zaspalis, E. A. Deliyanni, D. N. Bakoyannakis, E. N. Peleka, Hydrothermally prepared nanocrystalline Mn−Zn ferrites: Synthesis and characterization, Microporous and Mesoporous Materials 114 (2008) 465-473.

[19] J. Wang, C. Zeng, Z. M. Peng, Q. W. Chen, Synthesis and magnetic properties of $Zn_{1-x}Mn_xFe_2O_4$ nanoparticles, Physica B: Condensed Matter 349 (2004) 124-128.

[20] D. S. Mathew, R. S. Juang, An overview of the structure and magnetism of spinel ferrite nanoparticles and their synthesis in microemulsions, Chemical Engineering Journal 129 (2007) 51-65.

[21] S. Dasgupta, K. B. Kim, J. Ellrich, J. Eckert, I. Manna, Mechano-chemical synthesis and characterization of microstructure and magnetic properties of nanocrystalline $Mn_{1-x}Zn_xFe_2O_4$, Journal of alloys and compounds 424 (2006) 13-20.

[22] Raghvendra Singh Yadav, Jaromir Havlica, Ivo Kuritka, Zuzana Kozakova, Eva Bartonickova, Jiri Masilko, Lukas Kalina, Jaromir Wasserbauer, Miroslava Hajduchova, Vojtech Enev, Structural and Magnetic Properties of $CoFe_{2-x}Gd_xO_4$ ($0.0 \leq x \geq 0.1$) Spinel Ferrite Nanoparticles Synthesized by Starch-Assisted Sol–Gel Auto-combustion Method, Journal of Superconductivity and Novel Magnetism 28 (2015) 1797-1806.

5. List of Publications

❖ Journals

- **Prashant Thakur**, R. Sharma, V. Sharma, Pankaj Sharma. "*Structural and optical properties of $Mn_{0.5}Zn_{0.5}Fe_2O_4$ nano ferrites: Effect of sintering temperature*." **Materials Chemistry and Physics** 193 (2017) 285-289 (**SCI, Scopus Indexed, I.F. = 2.210**).

- **Prashant Thakur**, R. Sharma, V. Sharma, P. B. Barman, M. Kumar, D. Barman, S. C. Katyal, Pankaj Sharma. "*Gd^{3+} doped Mn-Zn soft ferrite nanoparticles: Superparamagnetism and its correlation with other physical properties*" **Journal of Magnetism and Magnetic Materials** 432 (2017) 208-217 (**SCI, Scopus Indexed, I.F. = 3.046**).

- **Prashant Thakur**, R. Sharma, M. Kumar, S. C. Katyal, N. S. Negi, N. Thakur, V. Sharma, Pankaj Sharma. "*Superparamagnetic La doped Mn–Zn nano ferrites: dependence on dopant content and crystallite size*" **Materials Research Express** 3(7) (2016) 075001 (**SCI, Scopus Indexed, I.F. = 1.151**).

- **Prashant Thakur**, R. Sharma, M. Kumar, V. Sharma, Pankaj Sharma. "*Structural, morphological, magnetic and optical study of Nd^{3+} doped Mn-Zn ferrite nanoparticles synthesized via co-precipitation technique*" (2018) (**Communicated to a SCI**, **Scopus Indexed Journal**).

❖ Paper presented in Conferences

- **Prashant Thakur**, R. Sharma, V. Sharma, Pankaj Sharma. "*Effect of Gd doping on the optical band gap of Mn-Zn nano ferrites*" National Seminar on Innovations & Challenges in Basic & Applied Sciences (ICBAS-2017) at Maharaja Agrasen University (H.P.) on March 04, 2017.

- **Prashant Thakur**, R. Sharma, V. Sharma, Pankaj Sharma. "*Structural and optical study of manganese zinc nano ferrite*" National Conference on Recent innovations in Applied Sciences and Humanities (NCASH-2015) at Rawal Institutions, Faridabad on October 10, 2015.

- **Prashant Thakur**, R. Sharma, V. Sharma, Pankaj Sharma. "*Effect of sintering temperature on structure and morphology of Mn-Zn soft ferrite*" International Conference on Emerging Trends in Basic & Applied Sciences at Maharaja Agrasen University (H.P.) on May 1-2, 2015.